Borole Derivatives. 22. Iodine Degradation of the Triple-Decker Complexes (μ-C_4H_4BR)[Rh(C_4H_4BR)]$_2$ (R = Ph, Me): Synthesis and Structural Characterization of Heterocubanes [Rh(μ_3-I)(C_4H_4BR)]$_4$ and of Bis(borole)rhodium Complexes RhI(C_4H_4BR)$_2$[1]

Gerhard E. Herberich,* Hartmut J. Eckenrath,[2] and Ulli Englert

Institut für Anorganische Chemie, Technische Hochschule Aachen, D-52056 Aachen, Germany

Received May 21, 1997[⊗]

The triple-decker complexes (μ-C_4H_4BR)[Rh(C_4H_4BR)]$_2$ (R = Ph, Me) (**1**) react with elemental iodine in toluene or dichloromethane to produce heterocubanes [Rh(μ_3-I)(C_4H_4BR)]$_4$ (**2**) and bis(borole)iodorhodium complexes RhI(C_4H_4BR)$_2$ (**3**). The heterocubanes **2** exchange fragments RhI(C_4H_4BR) at rates which are fast with respect to the NMR time scale. The bis(borole) compounds **3** exist in an equilibrium of rotational isomers C_s-**3** = C_{2v}-**3** with $\Delta_R H = (-1.7 \pm 0.2)$ kJ mol^{-1} and $\Delta_R S = (-16 \pm 1)$ J mol^{-1} K^{-1} for **3b**. Activation parameters for the forward and reverse isomerization reactions are reported. The isomerization takes place by the mechanism of ring−ring rotation; this is demonstrated for **3b** by TOCSY NMR spectra (^{1}H NMR, −80 °C, mixing time 150 ms). Crystal structure determinations of **2a**, **2b**, and **3b** are reported. The higher-energy isomer C_s-**3b** is found in the crystal of **3b**. One borole ligand of C_s-**3b** is planar and η^5-bonded with a normal Rh−B1 bond distance [236.7(6) pm]. The second ligand shows an unusual folding of 15.8(9)° along the line C2−C5, a very weak bonding interaction Rh−B2 [252.8(6) pm] approaching η^4-coordination, and a close contact I−B2 [295.3(6) pm]. Both borole ligands show diene-like C−C bond length patterns with weak Rh-to-borole back-bonding.

Introduction

In 1983 we found that dehydrogenative complex formation of 2,5-dihydro-1*H*-boroles provides an efficient and versatile route to *C*-unsubstituted (borole)metal complexes. Among the very first examples was the triple-decker complex (μ-C_4H_4BPh)[Rh(C_4H_4BPh)]$_2$ (**1a**),[3] and later the methyl analog **1b** was also described.[4] In this paper we report the oxidative degradation by iodine of the triple-decker complexes **1a**,**b**. This reaction will give us two new types of products, the dark red heterocubanes [Rh(μ_3-I)(C_4H_4BR)]$_4$ (**2**) and the orange bis(borole)iodorhodium compounds RhI(C_4H_4BR)$_2$ (**3**). Of these, the compounds **3** should attract particular attention because of a hitherto unknown bonding situation of a folded, approximately *tetrahapto*-coordinated borole ligand. In later papers we shall show that the complexes **2** are useful as versatile sources of the (borole)-rhodium fragments Rh(C_4H_4BR).

Results and Discussion

Syntheses. The triple-decker complexes **1a**,**b** readily react with elemental iodine. Two types of products **2** and **3** are obtained if toluene or CH_2Cl_2 is used as solvent at ambient temperature. The stoichiometry of this oxidation has been established in NMR tube experiments using d_8-toluene as solvent (Scheme 1).

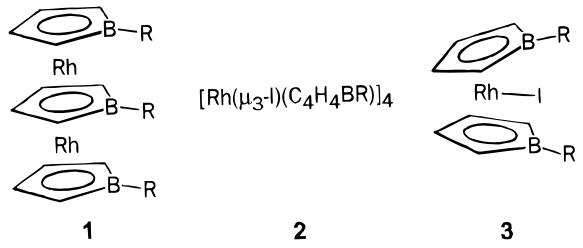

1 **2** **3**

9, R = Ph; **b**, R = Me

Scheme 1

(μ-C_4H_4Br)[Rh(C_4H_4BR)]$_2$ + I_2 → **1a,b**

$^1/_4$[Rh(μ_3-I)(C_4H_4BR)]$_4$ + RhI(C_4H_4BR)$_2$ **2a,b** **3a,b**

The two types of products **2** and **3** could not be separated by standard methods. When CO is bubbled through the reaction mixture, the heterocubanes **2** undergo a fast degradation (0.5 min, 20 °C) to form labile and more soluble carbonyl derivatives, the dicarbonyl RhI(CO)$_2$(C_4H_4BR) and dinuclear species [Rh(μ-I)(CO)(C_4H_4BR)]$_2$.[5] The bis(ligand) complexes **3** react with CO at ambient temperature with noticeable rates. At elevated temperature they decompose quantitatively (80 °C, 5−7 h); one of the two borole ligands is destroyed, and the formally remaining complex fragments are stabilized in the form of the same carbonyl species

[⊗] Abstract published in *Advance ACS Abstracts*, September 1, 1997.

(1) Part 21: Herberich, G. E.; Wagner, T.; Marx, H.-W. *J. Organomet. Chem.* **1995**, *502*, 67; **1996**, *513*, 287.

(2) Eckenrath, H. J. Doctoral Dissertation, Technische Hochschule Aachen, Aachen, Germany, 1997.

(3) Herberich, G. E.; Hessner, B.; Boveleth, W.; Lüthe, H.; Saive, R.; Zelenka, L. *Angew. Chem., Int. Ed. Engl.* **1983**, *22*, 996; *Angew. Chem. Suppl.* **1983**, 1503.

(4) Herberich, G. E.; Büschges, U.; Hessner, B.; Lüthe, H. *J. Organomet. Chem.* **1986**, *312*, 13.

(5) Herberich, G. E.; Eckenrath, H. J.; Englert, U. To be published.

S0276-7333(97)00422-6 CCC: $14.00

mentioned above. In the absence of CO the bis(ligand) complexes **3** decompose less selectively; inter alia the triple-decker compounds are also formed. Finally, when solutions of the carbonyl species are heated in a stream of dinitrogen (110 °C, 4−8 h) a clean decomposition takes place to produce the heterocubanes **2**.

With these observations in mind we were able to develop two practical variants. Carbonylation of the reaction mixture at ambient temperature solubilizes the less soluble complexes **2**; the bis(ligand) complexes **3** can then be isolated by crystallization at lower temperature. On the other hand, carbonylation at elevated temperature and subsequent thermal decarbonylation cleanly gives the heterocubanes **2** as the sole complex products (Scheme 2).

Scheme 2

$$(\mu\text{-}C_4H_4BR)[Rh(C_4H_4BR)]_2 + I_2 \xrightarrow{\text{i−iii}} {}^1/_2[Rh(\mu_3\text{-}I)(C_4H_4BR)]_4$$

1a,b **2a,b**

i, toluene 20 °C, 2 h; ii, CO (1 bar), 80 °C, 5−7 h; iii, N_2 stream, 110 °C, 4−8 h

An exploratory investigation of **1a** by cyclic voltammetry revealed a reversible reduction at −1.44 V vs SCE in DME and a fully irreversible oxidation at 1.19 V in CH_2Cl_2. Considering the high anodic potential for the oxidation, the ready degradation by iodine may seem surprising. The same apparently paradoxical situation is found in the chemistry of $Fe(CO)_5$.[6] On the basis of the redox potential of **1a** a one-electron oxidation by iodine is impossible. However, the basicity of the d^8 metal center favors an electrophilic attack at one Rh center. Thus we may speculate that a charge transfer adduct **1a**·I_2 and an ionic species [(**1a**)I]I (**4**) are likely intermediates. From earlier work we know (i) that triple-decker complexes with central borole ligands are prone to nucleophilic degradation,[4,7] and (ii) that cationic species are particularly reactive in this respect.[8] Thus we expect that the cation of **4** should readily undergo nucleophilic degradation by iodide; this degradation would produce **3** and, formally, the monomer of **2**.

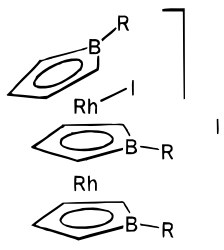

4

(6) Shriver, D. F.; Whitmire, K. H. In *Comprehensive Organometallic Chemistry*; Wilkinson, G., Stone, F. G. A., Abel, E. W., Eds.; Pergamon Press: Oxford, U.K., 1982; Vol. 4, p 250.

(7) (a) Herberich, G. E.; Büschges, U. *Chem. Ber.* **1989**, *122*, 615. (b) Herberich, G. E.; Hessner, B.; Saive, R. *J. Organomet. Chem.* **1987**, *319*, 9.

(8) Herberich, G. E.; Dunne, B. J.; Hessner, B. *Angew. Chem., Int. Ed. Engl.* **1989**, *28*, 737.

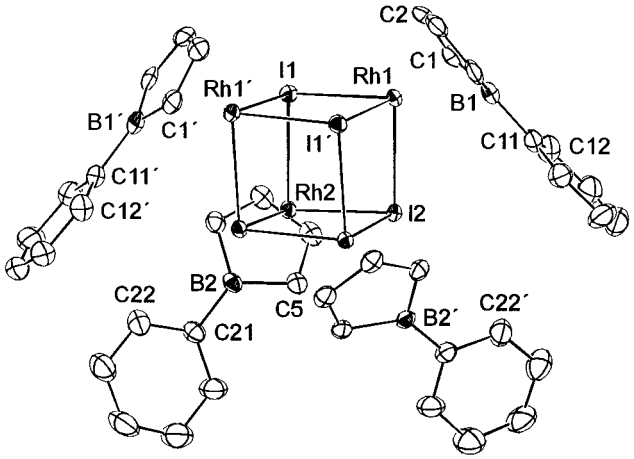

Figure 1. Thermal ellipsoid plot (ORTEP)[9] of the molecule **2a**. Ellipsoids are scaled to 30% probability.

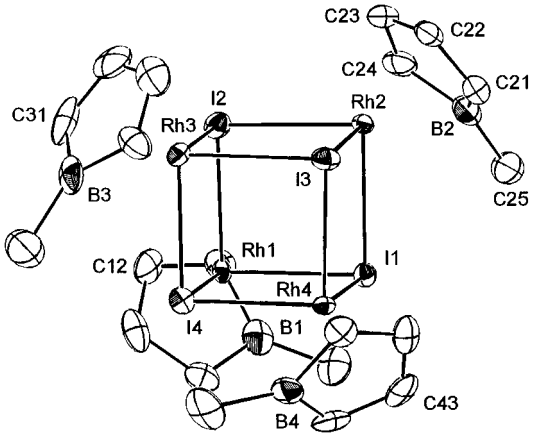

Figure 2. Thermal ellipsoid plot (ORTEP)[9] of the molecule **2b**. Ellipsoids are scaled to 30% probability.

Table 1. Selected Interatomic Distances and Bond Angles for 2a

(a) Bond Distances (pm)			
I1−Rh1	275.52(6)	I2−Rh1	276.07(5)
I1−Rh1′	273.56(6)	I2−Rh2	272.80(5)
I1−Rh2	277.41(5)	I2−Rh2′	276.20(5)
Rh1−C1	217.1(6)	Rh2−C5	214.2(6)
Rh1−C2	212.9(6)	Rh2−C6	211.4(6)
Rh1−C3	209.5(6)	Rh2−C7	212.3(6)
Rh1−C4	215.4(6)	Rh2−C8	216.5(5)
Rh1−B1	229.8(7)	Rh2−B2	233.3(6)
(b) Bond Angles (deg)			
Rh1−I1−Rh1′	92.47(2)	Rh1−I2−Rh2	94.52(2)
Rh1−I1−Rh2	93.61(2)	Rh1−I2−Rh2′	91.00(2)
Rh1′−I1−Rh2	91.27(2)	Rh2−I2−Rh2′	90.44(1)
I1−Rh1−I1′	87.43(2)	I1−Rh2−I2	86.05(2)
I1−Rh1−I2	85.79(2)	I1−Rh2−I2′	88.29(2)
I1′−Rh1−I2	89.10(2)	I2−Rh2−I2′	89.41(1)

Crystal Structures of the Heterocubanes 2a and 2b. Both complexes **2a**,**b** display a heterocubane structure with a Rh_4I_4 core (Figures 1 and 2, Tables 1 and 2). Complex **2a** crystallizes in space group *C*2/*c* and compound **2b** in *Pbca*. The molecules of **2a** possess crystallographic C_2 symmetry.

The Rh−I bond lengths average 275.8 pm [range: 270.49(9)−281.1(1) pm]. This is slightly longer than in the many known structures with μ_2-iodo ligands;[10] structures with μ_3-iodo ligands are apparently unknown for rhodium. The angles centered at rhodium average 87.7° [range: 85.11(3)−91.70(3)°], and those centered

Table 2. Selected Interatomic Distances and Bond Angles for 2b

(a) Bond Distances (pm)			
I1−Rh1	276.5(1)	I2−Rh1	270.49(9)
I1−Rh2	276.2(1)	I2−Rh2	275.8(1)
I1−Rh4	274.8(1)	I2−Rh3	276.8(1)
I3−Rh2	277.7(1)	I4−Rh1	281.1(1)
I3−Rh3	273.8(1)	I4−Rh3	279.85(9)
I3−Rh4	276.29(9)	I4−Rh4	276.54(9)
(b) Bond Angles (deg)			
Rh1−I1−Rh2	87.74(3)	Rh1−I2−Rh2	89.03(3)
Rh1−I1−Rh4	94.57(3)	Rh1−I2−Rh3	95.93(3)
Rh2−I1−Rh4	93.60(3)	Rh2−I2−Rh3	91.47(3)
Rh2−I3−Rh3	91.71(3)	Rh1−I4−Rh3	92.88(3)
Rh2−I3−Rh4	92.93(3)	Rh1−I4−Rh4	93.15(3)
Rh3−I3−Rh4	92.26(3)	Rh3−I4−Rh4	90.91(3)
I1−Rh1−I2	91.70(3)	I1−Rh2−I2	90.63(3)
I1−Rh1−I4	85.53(3)	I1−Rh2−I3	86.45(3)
I2−Rh1−I4	86.05(3)	I2−Rh2−I3	88.06(3)
I2−Rh3−I3	88.67(3)	I1−Rh4−I3	87.01(3)
I2−Rh3−I4	85.11(3)	I1−Rh4−I4	86.75(3)
I3−Rh3−I4	88.06(3)	I3−Rh4−I4	88.23(3)

at iodine average 92.2° [range: 87.74(3)−95.93(3)°]. The cubane faces are almost perfectly planar (the angle sums deviating from 360° by at most 0.9°).

The structural pattern of the borole ligands is similar to that established in earlier structural work, as, e.g., in $RhCl(C_4H_4BPh)(PPh_3)_2$,[11] $Fe(CO)_3(C_4H_4BPh)$,[12] and $(\mu\text{-}C_4H_4BMe)[Co(C_4H_4BMe)]_2$,[7b] and will not be discussed in detail. The distance of the Rh atoms to the best borole planes ranges from 177.4 to 178.3 pm while the Rh−B bond lengths average 232.5 pm, in agreement with η^5-coordination of the borole ligand.

The observation of a heterocubane structure for **2a**,**b** may seem surprising at first glance. The related complexes of the types $[RhX(alkene)_2]_2$ and $[RhX(diene)]_2$ (X = halogen) are *dinuclear square planar* complexes of a predominantly d^8 metal center.[13] The tetrafluoroethene complex $[RhF(C_2H_4)(C_2F_4)]_x$ is an exception; it shows a "dimer-of-dimer" structure in the crystal but is a dimer in solution.[14] As a consequence of the very strong back-bonding ability of the C_2F_4 ligand, the metal assumes more d^6 character and the 18e configuration becomes more favorable. In the borole complexes **2a**,**b** the strong back-bonding ability of the borole ligand[15] results in pronounced metal−ligand orbital mixing,[16] and a description as d^8 complexes is no longer appropriate. Thus, the compounds **2a**,**b** seem more akin to complexes such as $[Cp^*RuCl]_4$,[17] to which they are isoelectronic in a broad sense.

(9) Johnson, C. K. Oak Ridge National Laboratory ORNL-5138 (Third Revision, 1976).
(10) Orpen, A. G.; Brammer, L.; Allen, F. H.; Kennard, O.; Watson, D. G.; Taylor, R. *J. Chem. Soc., Dalton Trans.* **1989**, S1.
(11) Herberich, G. E.; Boveleth, W.; Hessner, B.; Hostalek, M.; Köffer, D. P. J.; Negele, M. *J. Organomet. Chem.* **1987**, *319*, 311.
(12) Herberich, G. E.; Boveleth, W.; Hessner, B.; Köffer, D. P. J.; Negele, M.; Saive, R. *J. Organomet. Chem.* **1986**, *308*, 153.
(13) Hughes, R. P. In *Comprehensive Organometallic Chemistry*; Wilkinson, G., Stone, F. G. A., Abel, E. W., Eds.; Pergamon Press; Oxford, 1982; Vol. 5, p 277, especially p 418, 445, 447, and 456.
(14) Burch, R. R.; Harlow, R. L.; Ittel, S. D. *Organometallics* **1987**, *6*, 982.
(15) Herberich, G. E.; Carstensen, T.; Köffer, D. P. J.; Klaff, N.; Boese, R.; Hyla-Kryspin, I.; Gleiter, R.; Stephan, M.; Meth, H.; Zenneck, U. *Organometallics* **1994**, *13*, 619 and literature cited therein.
(16) (a) Hyla-Kryspin, I.; Gleiter, R.; Herberich, G. E.; Bénard, M. *Organometallics* **1994**, *13*, 1795. (b) Gleiter, R.; Hyla-Kryspin, I.; Herberich, G. E. *J. Organomet. Chem.* **1994**, *478*, 95.
(17) Fagan, P. J.; Mahoney, P. S.; Calabrese, J. C.; Williams, I. D. *Organometallics* **1990**, *9*, 1843.
(18) Spek, A. L. *Acta Crystallogr.* **1990**, *A46*, C34.

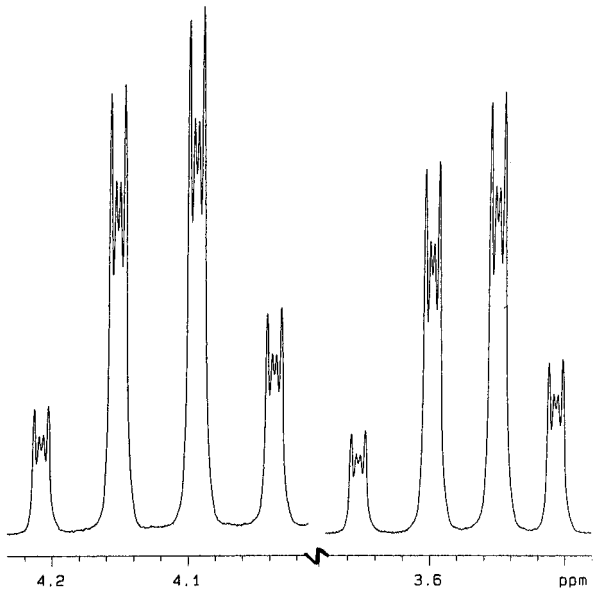

Figure 3. Low-temperature ^1H NMR signals (500 MHz, CD_2Cl_2, −80 °C) of a **2a**/**2b** mixture (1.20/1) in the borole region.

Constitution of 2a and 2b in Solution. The heterocubanes **2a**,**b** readily undergo degradation reactions with a wide variety of Lewis bases such as, e.g., CO, acetonitrile, pyridine, and phosphines.[2,5] The carbonylation is reversible, and solutions of **2a**,**b** in acetonitrile regenerate the heterocubanes upon removal of the solvent in a vacuum.

Osmometric determinations of the molar mass of **2a** in CH_2Cl_2 give values somewhat below the value calculated for the heterocubane structure. These measurements confirm that **2a** essentially retains its tetranuclear nature in CH_2Cl_2 solution. On the other hand, they may be taken as a hint that **2a** does undergo a dissociation in solution, presumably into the dinuclear species. ^1H NMR spectra in $CDCl_3$ taken at ambient temperature on an 80 MHz spectrometer display one set of sharp signals consisting of the typical AA′BB′ pattern of a coordinated borole ligand and the signals of the group R. The same spectra taken on a 500 MHz spectrometer show broad pseudosinglets in the region of the AA′BB′ signals. The signals sharpen at higher temperature (d_8-toluene, 80 °C) and also upon cooling down to −80 °C.

To get more insight we looked at mixtures of **2a** and **2b** and measured their ^1H NMR spectra in CD_2Cl_2. Spectra taken at room temperature and at 80 MHz display only two ligand patterns corresponding to a 1-methyl- and a 1-phenylborole ligand; again, the spectra are blurred when measured at 500 MHz. At −80 °C, low-temperature limiting spectra with several different borole ligand patterns are seen, two of which are those of **2a** and **2b** (Figure 3). The spectra could be simulated with the assumption that five species $Rh_4(\mu_3\text{-}I)_4(C_4H_4BMe)_{4-x}(C_4H_4BPh)_x$ (with x = 0, 1, ..., 4) are present, with relative concentrations which correspond to statistical weights of the five species. The essential result is the proof that heterocubanes **2** exchange fragments $RhI(C_4H_4BR)$ at rates which are fast with respect to the NMR time scale under the common experimental conditions.

Crystal Structure of the Bis(ligand) Complex 3b. Complex **3b** crystallizes in the monoclinic space group

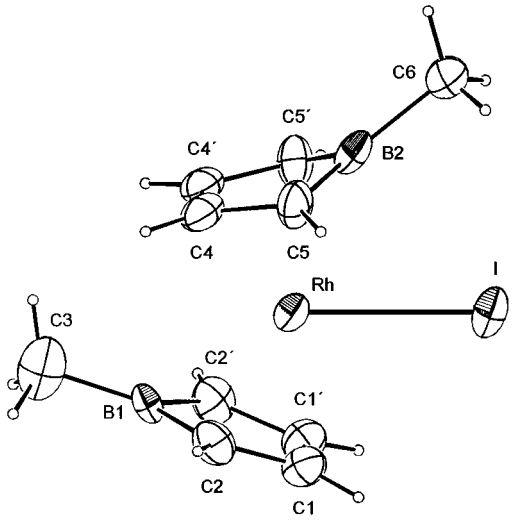

Figure 4. Thermal ellipsoid plot (PLATON)[18] of the molecule C_s-**3b**. Ellipsoids are scaled to 30% probability.

Table 3. Selected Interatomic Distances and Bond Angles for 3b

(a) Bond Distances (pm)			
I−Rh	273.51(5)	I−B2	295.3(6)
Rh−C1	217.2(3)	Rh−C4	216.0(3)
Rh−C2	224.8(4)	Rh−C5	223.5(4)
Rh−B1	236.7(6)	Rh−B2	252.8(6)
C1−C1′	146.2(8)	C1−C2	138.7(5)
C2−B1	155.3(6)	C3−B1	155.8(9)
C4−C4′	143.4(8)	C4−C5	139.9(5)
C5−B2	156.3(6)	C6−B2	155.6(9)
(b) Bond Angles (deg)			
C1′−C1−C2	109.7(2)	C4′−C4−C5	110.2(2)
C1−C2−B1	109.7(4)	C4−C5−B2	108.3(4)
C2−B1−C2′	101.2(5)	C5−B2−C5′	100.3(5)
C2−B1−C3	129.4(2)	C5−B2−C6	129.1(2)

*C*2/m. The molecule of **3b** possesses a bent sandwich structure with crystallographic C_s symmetry (Figure 4, Table 3). The tight packing of the ligands around the Rh center is illustrated by a space-filling representation (Figure 5). The Rh−I bond length amounts to 273.51(5) pm and lies in the expected range.[10] One of the two borole ligands shows structural features similar to those found in $RhCl(PPh_3)_2(C_4H_4BPh)$.[11] This ring is planar [plane C1,C1′,C2,C2′,B1; largest vertical displacement: 1.5(6) pm at B1]. The boron atom B1 is slightly bent away from the metal [vertical distance to plane C1,C1′,C2,C2′: 4.2(6) pm], yet B1 is a trigonal planar center [angle sum 360.0(5)°]. The metal-to-ring bonding shows a vertical distance of the Rh atom to the best borole plane of 185.8(1) pm, a rather large slip distortion of 13.7(3) pm,[19] and a Rh−B1 distance of 236.7(6) pm [cf. Rh−B 232.5 pm (av) for **2a** and **2b**; cf. also $RhCl(PPh_3)_2(C_4H_4BPh)$:[11] slip distortion 11.5 pm, Rh−B 240.0(5) pm]. The C−C bond lengths in the ring [C1−C1′ 146.2(8), C1−C2 138.7(5) pm] show a diene-like pattern, indicating rather moderate back-bonding.

The second ring shows surprising structural features. The folding angle between the two planes C5,B2,C5′ and C5,C4,C4′,C5′ of 15.8(9)° is exceptionally large, resulting in rather weakened bonding between the Rh atom and B2 [Rh−B2 252.8(6) pm]; the vertical distances to the diene plane C4,C4′,C5,C5′ amount to 27.2(7) pm for B2 and to 183.7(1) pm for the Rh atom. Thus the bonding situation is approaching a *tetrahapto*-coordination of the borole ligand. The orientation of this ring brings the boron atom B2 into contact with the iodine atom. The distance I···B2 [295.3(6) pm] is much larger than typical B−I bond lengths [BI_3·PMe_3: 223.7(9) and 227.2(16) pm[20]] but also much shorter than a nonbonding distance [>360 pm].[21] The boron center is no longer trigonal planar. The methyl group is bent away from the metal, and the angle between the plane C5,B2,C5′ and the bond vector B2−C6 amounts to 10.5(2)°. The resulting distance I···C of the *B*−Me group [335.0(7) pm] corresponds to an at most very weak repulsion. Finally, the C−C distances in the ring [C4−C4′ 143.4(8), C4−C5 139.9(5) pm] show again a diene-like pattern with moderate back-bonding.

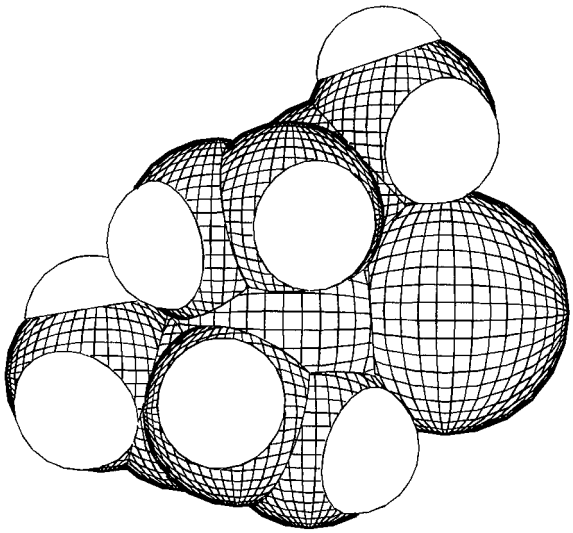

Figure 5. Space-filling representation (PLATON)[18] of the molecule C_s-**3b**.[18]

Overall, two effects seem to be operating here, pronounced ligand−ligand repulsions and a weak bonding interaction between the boron center B2 and the iodo ligand. However, the origin of the slight pyramidalization at B2 remains unclear since both the I···B2 interaction and the distance I···C of the *B2*-Me group are in the borderline range.

Structures of 3a,b in Solution. The ^1H and ^{13}C NMR spectra of **3a**,**b** at ambient temperature display only one borole pattern, and some atoms show signal broadening which cannot be caused by the quadrupole moment of a neighboring boron atom [**3a**, 3-/4-H, C-3,4; **3b**, C-3,4]. We therefore measured NMR spectra at temperatures down to −90 °C with the aim to unravel the dynamic behavior of the complexes **3**.

The low-temperature limiting ^1H NMR spectrum of **3b** shows six multiplets in the region of the borole rings, four of equal intensity and a pair of somewhat lower intensity (Figure 6). With the help of (^1H,^1H)-COSY spectra (taken at −90 °C) these multiplets can be grouped into three AA′BB′ patterns; the presence of an ABCD spin system can be excluded unambiguously. The two AA′BB′ systems of equal intensity are assigned to the isomer C_s-**3b** found in the crystal while the third one is assigned to an isomer C_{2v}-**3b**. Since the borole

(19) The slip distortion is the distance between the geometric center of the C_4B ring and the projection of the metal atom onto the C_4B best plane.

(20) Black, D. L.; Taylor, R. C. *Acta Crystallogr.* **1975**, *B31*, 1116.
(21) van der Waals radii: Bondi, A. *J. Phys. Chem.* **1964**, *68*, 441.

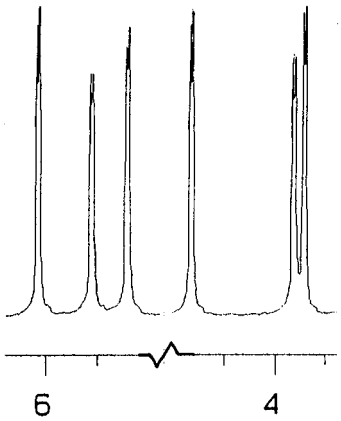

Figure 6. Low-temperature ^{1}H NMR signals (500 MHz, CD_2Cl_2, −90 °C) of **3b** in the borole region.

Scheme 3[a]

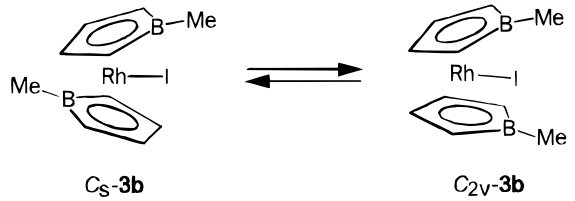

C_s-**3b** C_{2v}-**3b**

[a] C_s-**3b** ⇌ C_{2v}-**3b**.

Table 4. Equilibrium Constants and Free Energies for the Equilibrium C_s-3b ⇌ C_{2v}-3b

T (K)	C_{2v}-**3b**/C_s-**3b**[a]	K	$\Delta_R G$ (kJ mol^{-1})
183	30/70	0.43	1.284
193	29/71	0.41	1.430
203	28/72	0.39	1.589
213	27/73	0.38	1.714
223	26/74	0.35	1.946

[a] The concentration ratios rely on the assumption that the intensities of corresponding signals in the $^{13}C\{^1H\}$ NMR spectrum are comparable.

Table 5. Energetics of the Equilibrium C_s-3 ⇌ C_{2v}-3

(a) Thermodynamic Equilibrium Parameters for **3b**
$\Delta_R H = (-1.7 \pm 0.2)$ kJ mol^{-1}
$\Delta_R S = (-16 \pm 1)$ J mol^{-1} K^{-1}

(b) Activation Parameters for Isomerization of C_s-**3b**
$\Delta H^{\ddagger}_1 = (34.0 \pm 1.9)$ kJ mol^{-1}
$\Delta S^{\ddagger}_1 = (-47 \pm 9)$ J mol^{-1} K^{-1}

(c) Activation Parameters for Isomerization of C_{2v}-**3b**
$\Delta H^{\ddagger}_{-1} = (35.6 \pm 2.0)$ kJ mol^{-1}
$\Delta S^{\ddagger}_{-1} = (-32 \pm 9)$ J mol^{-1} K^{-1}

(d) Activation Parameters for Isomerization of C_s-**3a**
$\Delta H^{\ddagger} = (33.5 \pm 1.5)$ kJ mol^{-1}
$\Delta S^{\ddagger} = (-52 \pm 7)$ J mol^{-1} K^{-1}

patterns coalesce at higher temperature and sharpen to the single pattern seen at ambient temperature, the two isomers are in a mobile equilibrium (Scheme 3). Note that isomer C_{2v}-**3b** is shown as a syn-eclipsed conformer with both BMe groups close to the Rh−I bond; the alternative anti-eclipsed conformer would seem too congested sterically to be capable of existence.

Signal intensities of corresponding signals in the $^{13}C\{^1H\}$ NMR spectra were used to estimate equilibrium constants (Table 4) and to calculate thermodynamic parameters for the isomerization of Scheme 3 (Tables 4 and 5). Thus we obtained $\Delta_R H = (-1.7 \pm 0.2)$ kJ mol^{-1} and $\Delta_R S = (-16 \pm 1)$ J mol^{-1} K^{-1}. This result shows that the lower-energy isomer is C_{2v}-**3b** while the less symmetric C_s-**3b** is entropically favored and predominates in the entire temperature range that is accessible experimentally.

When a 500 MHz ^{1}H NMR spectrum of the phenyl compound **3a** is measured at −90 °C, the low-temperature limiting spectrum for C_s-**3a** with resolved fine structure is observed while the borole signals for C_{2v}-**3a** are seen as a pair of weak broad pseudosinglets. In the $^{13}C\{^1H\}$ NMR spectrum (126 MHz, −90 °C) only the signals of C_s-**3a** could be observed. The equilibrium constant is about $K \approx 0.1$, corresponding to $\Delta_R G_{183} = 3.5$ kJ mol^{-1}.

The room temperature $^{11}B\{^1H\}$ NMR spectrum of **3b** displays a single resonance for the equilibrium mixture at δ 33 ppm while the low-temperature limiting spectrum (160 MHz, −80 °C) shows a more intense signal at δ 37 and a weaker signal at δ 28 ppm. The chemical shift of the weaker signal corresponds to a normal 1-methylborole ligand in a situation with rather moderate back-bonding,[22] and is therefore assigned to the planar borole ring of C_s-**3b**. The chemical shift of the stronger signal is very unusual and indicates considerable deshielding at the boron; it belongs to the folded borole ring of C_s-**3b** and, because of its higher intensity, also to the borole rings of C_{2v}-**3b**. Thus, we have to conclude that both borole rings in C_{2v}-**3b** are of the folded type with weakened Rh−B bonding. In the case of **3a** no splitting of the signal was seen at −80 °C.

We next turn to the mechanism of the forward and reverse isomerization reactions. Since the coalescence temperatures observed are concentration-independent, the isomerization processes are first-order reactions. Line shape analysis with the help of the program DNMR[24] was used to estimate isomerization rates and to calculate activation parameters for both isomers of **3b** and for the predominant isomer C_s-**3a** in the phenyl case (Table 5). The negative activation entropies obtained demonstrate the nondissociative and consequently intramolecular nature of the reactions observed. We conclude that the isomerization is brought about by ring−ring rotation.

This mechanism can be verified directly by means of the TOCSY NMR spectra[25] of **3b**. The spectra were recorded at −80 °C with a mixing time of 150 ms. We describe selective excitations of borole protons in β-positions to the boron (i.e., 3-/4-H) and the transfer of magnetization to β-positions in the other borole rings; α-protons (i.e., 2-/5-H) and transfer of magnetization to these positions can remain out of consideration. Selective excitation of the β-protons of one borole in C_s-**3b** produces a strong signal for these protons, a less intensive signal for the β-protons in C_{2v}-**3b**, and an even less intensive signal for the β-protons of the second borole in C_s-**3b**. Thus the interconversion of the two borole ligands of C_s-**3b** takes place through the intermediacy of isomer C_{2v}-**3b**. On the other hand, if the β-protons of C_{2v}-**3b** are excited selectively, then both β-proton signals of C_s-**3b** appear with equal intensity.

(22) Cf., e.g., δ 28.5 ppm for $Ni(C_4H_4BMe)_2$[23] and also δ 19.6 for $CpRh(C_4H_4BMe)$[4] and 22.8 ppm for $Ru(CO)_3(C_4H_4BMe)$.[11]

(23) Herberich, G. E.; Negele, M. *J. Organomet. Chem.* **1988**, *350*, 81.
(24) Haegele, G.; Lenzen, T.; Fuhler, R. *Comput. Chem.* **1995**, *19*, 277.
(25) Braunschweiler, L.; Ernst, R. R. *J. Magn. Reson.* **1983**, *53*, 521.

Barriers to internal rotation of borole ligands have previously been observed.[23,26] We note that the present case is the first nondegenerate example that could be analyzed.

Concluding Remarks. In this paper we have concentrated on the oxidative degradation reaction of the triple-decker complexes **1** and the identification and the structures of the products **2** and **3**. For the preparation of the heterocubanes **2** we have devised an optimized procedure which circumvents the separation of the products **2** and **3** and gives the heterocubanes **2** as the sole product in high yields (80−85%). In the next paper of this series we shall describe reactions of the heterocubanes **2** with a wide variety of Lewis bases. We shall then be able to comment in detail on the role of CO, acetonitrile, and pyridine in the oxidative degradation reaction.

Experimental Section

General Procedures. Reactions were carried out under an atmosphere of dinitrogen by means of conventional Schlenk techniques. Hexane was distilled from potassium, CH_2Cl_2 from CaH_2, and toluene from sodium. Acetone was heated under reflux with boric acid anhydride for 24 h and distilled under dinitrogen. Acetonitrile was filtered through a column with activated alumina and distilled under dinitrogen. Carbon monoxide was dried with concentrated sulfuric acid. NMR spectra were recorded on a Varian Unity 500 spectrometer (^{1}H, 500 MHz; ^{13}C{^{1}H}, 125.7 MHz; ^{11}B{^{1}H}, 160.4 MHz) and a Bruker WP-80 PFT (^{1}H, 80 MHz) spectrometer. If not stated otherwise, chemical shifts were measured at ambient temperature and are relative to internal TMS for ^{1}H and ^{13}C and relative to $BF_3{\cdot}Et_2O$ as external reference for ^{11}B. The *B*-phenyl compounds **2a** and **3a** are poorly soluble in noncoordinating solvents such as toluene or CH_2Cl_2; this was frequently a limiting factor in the recording of NMR spectra.

Secondary ion mass spectra (SIMS) were recorded on a Finnigan MAT-95 spectrometer. Elemental analyses and determinations of molecular mass were performed by Mikroanalytisches Labor Pascher, D-53424 Remagen-Bandorf, Germany. Melting points were determined in sealed capillaries on a Büchi 510 melting point apparatus and are uncorrected.

CV Data of 1a. Cyclic voltammetry was carried out using an EG & G 175 voltage scan generator and an EG & G 173 potentiostat. For the measurements a conventional three-electrode cell with a platinum-inlay working electrode, a platinum sheet counter electrode, and a saturated calomel (SCE) reference electrode was used. Solutions were ca. 10^{-3} M in electroactive species and 0.1 M in tetrabutylammonium hexafluorophosphate (TBAH) as supporting electrolyte. $FeCp_2$ served as internal standard. CV (CH_2Cl_2, 100 mV/s) E_p^a +1.19 V, irreversible oxidation; (DME, 100 mV/s) $E_{1/2}$ −1.44 V, i_a/i_c 0.99, reversible reduction.

Synthesis of [Rh(μ_3-I)(C_4H_4BPh)]$_4$ (2a). Elemental iodine (2.19 g, 8.629 mmol) was added to a solution of **1a**[3,4] (5.40 g, 8.63 mmol) in toluene (700 mL). The dark red reaction mixture was stirred at 20 °C for 2 h. Then a slow stream of dry CO was passed through the flask while the temperature was kept at 80 °C for 7 h. Then the orange solution was heated under gentle reflux while a slow stream of N_2 was passed through the flask until the CO band at 2055 cm^{-1} had disappeared. After cooling to 20 °C the volatiles were removed under reduced pressure. The raw product was suspended in acetone (30 mL), transferred to a frit, and washed with acetone until the color of the filtrate was of a pale red. The solid was then dissolved in hot acetonitrile (400 mL), the solution was filtered, and the solvent was removed in a vacuum. The microcrystals so obtained were collected on a frit, washed with acetone, and dried in a vacuum to give **2a** (5.31 g, 85%) as dark red microcrystals: mp 223 °C dec; in solution somewhat air-sensitive, soluble in acetonitrile, moderately soluble in CH_2Cl_2, $CHCl_3$, THF, and toluene, insoluble in acetone, ether, and hexane. Anal. Calcd for $C_{40}H_{36}B_4I_4Rh_4$: C, 32.48; H, 2.45. Found: C, 32.35; H, 2.50. Molar mass: M_{calc} 1479.21 g mol^{-1}; in acetonitrile M_{obs} [molarity (g/L)] 391 (5.548), 445 (11.77), 464 g/mol (13.05); in CH_2Cl_2 M_{obs} [molarity (g/L)] 1351 (3.475), 1430 g/mol (5.313). SIMS (DMBA): negative ions, m/z (I_{rel}) 1110 (1, $[Rh_3I_3(C_4H_4BPh)_3]^-$), 740 (8, $[Rh_2I_2(C_4H_4BPh)_2]^-$), 497 (70, $[RhI_2(C_4H_4BPh)]^-$), 357 (26, $[RhI_2]^-$), 127 (100, I^-).

2a: ^{1}H NMR (500 MHz, $CDCl_3$) δ 7.63 (m, 2 H_o), 7.37 (m, H_p), 7.35 (m, 2 H_m), borole 5.03 (br, 3-/4-H), 4.18 (br, 2-/5-H), and borole signals at 80 MHz 5.03 (m, N = 5.9 Hz, 3-/4-H), 4.18 (m, N = 5.2 Hz, 2-/5-H). ^{13}C{^{1}H} NMR (126 MHz, $CDCl_3$, 20 °C) δ 135.91 (C_o), 129.14 (C_p), 127.62 (C_m), borole 89.22 (C-3,4), 74 (br, C-2,5); ^{11}B{^{1}H} NMR ($CDCl_3$) δ 20.

Synthesis of [Rh(μ_3-I)(C_4H_4BMe)]$_4$ (2b). A solution of complex **1b**[4] (310 mg, 0.705 mmol) and elemental iodine (179 mg, 0.705 mmol) in toluene (100 mL) was stirred at 20 °C for 2 h. Carbonylation (5 h) and decarbonylation (4 h) until the CO band at 2059 cm^{-1} had disappeared, followed by removal of the volatiles, gave a raw product. This was dissolved in CH_2Cl_2 (80 mL), and the solution was filtered, concentrated to a small volume (3 mL), and stored at −30 °C for 16 h. The dark red microcrystals formed were collected, washed wih acetone (2 × 2 mL), and dried in a vacuum to give **2b** (350 mg, 81%): mp 168 °C dec; in solution somewhat air-sensitive, soluble in acetonitrile, CH_2Cl_2, $CHCl_3$, THF, and toluene, insoluble in acetone, ether, and hexane. Anal. Calcd for $C_{20}H_{28}B_4I_4Rh_4$: C, 19.52; H, 2.29. Found: C, 19.52; H, 2.23. SIMS (K/T): negative ions, m/z (I_{rel}) 743 (13, $[Rh_2I_3(C_4H_4BMe)_2]^-$), 616 (12, $[RhI(C_4H_4BMe)]_2^-$), 435 (62, $[RhI_2(C_4H_4BMe)]^-$), 127 (100, I^-).

2b: ^{1}H NMR (500 MHz, $CDCl_3$) δ 5.09 (br, 3-/4-H), 3.66 (br, 2-/5-H), 0.50 (s, Me), and borole signals at 80 MHz 5.10 (m, N = 5.2 Hz, 3-/4-H), 3.67 (m, N = 5.2 Hz, 2-/5-H). ^{13}C{^{1}H} NMR (126 MHz, $CDCl_3$) δ 88.44 [d, ^1J(Rh−C) = 8.8 Hz, C-3,4], 73.51 (br, C-2,5), −1.91 (br, Me). ^{11}B{^{1}H} NMR ($CDCl_3$) δ 24.

Synthesis of RhI(C_4H_4BPh)$_2$ (3a). Complex **1a**[3,4] (520 mg, 0.831 mmol) was dissolved in CH_2Cl_2 (50 mL), and elemental iodine (211 mg, 0.831 mmol) was added. The reaction mixture was stirred for 2 h at ambient temperature. Dry CO was then passed through the flask for 15 min. The orange solution was concentrated to 5 mL under reduced pressure and then stored at −30 °C for 16 h to give orange crystals. After removal of the mother liquor, dissolution in CH_2Cl_2 (30 mL), and filtration, the solution was again concentrated to 3 mL under reduced pressure and stored at −30 °C for 16 h. The crystals were collected on a frit, washed with acetone (3 × 2 mL), and dried in a vacuum to give **3a** (270 mg, 64%) as orange needles: mp 168 °C dec; in solution somewhat sensitive, moderately soluble in CH_2Cl_2, $CHCl_3$, and toluene, insoluble in acetone, acetonitrile, ether, and hexane. Anal. Calcd for $C_{20}H_{18}B_2IRh$: C, 47.12; H, 3.56. Found: C, 47.08; H, 3.39. SIMS (NBA): positive ions, m/z (I_{rel}) 626 (<1, $[Rh_2(C_4H_4BPh)_3]^-$), 383 (100, $[Rh(C_4H_4BPh)_2]^+$).

3a: ^{1}H NMR (500 MHz, CD_2Cl_2) δ 7.70 (m, 2 H_o), 7.41 (m, 2 H_m), 7.33 (m, H_p), borole 5.88 (br, 3-/4-H), 4.70 (m, 2-/5-H), and borole signals at 80 MHz 5.88 (m, N = 7.3 Hz, 3-/4-H), 4.71 (m, N = 6.8 Hz, 2-/5-H); ^{13}C{^{1}H} NMR (126 MHz, CD_2Cl_2) δ 136.36 (C_o), 130.54 (C_p), 128.28 (C_m), borole 103.74 (br, C-3,4), 81.47 (br, C-2,5). ^{11}B{^{1}H} NMR (CD_2Cl_2) δ 28.

VT-NMR spectra of 3a: ^{1}H NMR (500 MHz, CD_2Cl_2, −90 °C) C_s isomer (90%) δ 7.84 (m, 2 H_o), 7.53 (m, 2 H_o), 7.43−7.49 (m, 2 H_m + H_p), 7.33 (m, 2 H_m), 7.20 (m, H_p), 6.29 (m, 3-/4-H) and 4.93 (m, 2-/5-H) for first borole, 5.33 (m, 3-/4-H) and 4.45 (m, 2-/5-H) for second borole; C_{2v} isomer (10%) δ 6.02 (s br, 3-/4-H), 4.52 (s br, 2-/5-H), Ph protons hidden. ^{13}C{^{1}H} NMR

(26) (a) Herberich, G. E.; Negele, M.; Ohst, H. *Chem. Ber.* **1991**, *124*, 25. (b) Herberich, G. E.; Englert, U.; Hostalek, M.; Laven, R. *Chem. Ber.* **1991**, *124*, 17.

Table 6. Crystal Data, Data Collection Parameters, and Convergence Results

	2a	2b	3b
formula	$C_{40}H_{36}B_4I_4Rh_4$	$C_{20}H_{28}B_4I_4Rh_4$	$C_{10}H_{14}B_2IRh$
system	monoclinic	orthorhombic	monoclinic
space group (no.)	*C*2/*c* (15)	*Pbca* (61)	*C*2/*m* (12)
a, pm	1572.6(9)	1692.8(5)	993.6(4)
b, pm	1387.4(5)	1706.2(2)	891.4(3)
c, pm	1956.1(5)	2015.6(3)	1414.0(3)
β, deg	105.56(4)	2015.6(3)	104.55(3)
V, nm^3	4.112(3)	5.822(2)	1.2123(7)
Z	4	8	4
d_{calc}, g cm^{-3}	2.371	2.809	2.112
T, K	203	293	203
μ, cm^{-1}	4521	33.65	38.65
λ, pm (radiation)	71.073 (Mo Kα)	56.087 (Ag Kα)	71.073 (Mo Kα)
θ_{max}, deg	28	24	28
cryst dimens, mm^3	0.19 × 0.14 × 0.12	0.25 × 0.20 × 0.08	0.35 × 0.26 × 0.05
abs cor	numerical	empirical	numerical
min trans	0.442	rel 0.606	0.395
max trans	0.622	rel 0.999	0.899
no. of reflns	6143	10 799	5820
no. of indep obs rflns $I > 1.0\sigma(I)$	3712	5555	1311
no. of vars	236	290	104
R^a	0.035	0.070	0.028
$R_w{}^b$	0.036	0.055	0.032
resd el dens, 10^{-6} e pm^{-3}	0.8	1.8 (close to Rh)	1.1 (close to I)

$^a R = \sum||F_o| - |F_c||/\sum|F_o|$. $^b R_w = [\sum w(|F_o| - |F_c|)^2/\sum w|F_o|^2]^{1/2}$.

(126 MHz, $CDCl_3$, −90 °C) C_s isomer δ 135.30 and 135.80 (C_o), 127.14 and 127.94 (C_m), 129.86 and 130.02 (C_p), borole 100.88 and 106.99 (C-3,4), 75.35 and 85.55 (C-2,5); C_{2v} isomer not observed. Simulation of line shapes: temperature range 193−303 K; signals of borole carbons C-3,4 and of phenyl carbons C_o, C_m, and C_p used.

Synthesis of RhI($C_4H_4BMe)_2$ (3b). A solution of complex **1b**[4] (840 mg, 1.911 mmol) and elemental iodine (485 mg, 1.911 mmol) in CH_2Cl_2 (50 mL) was stirred at ambient temperature for 2 h. The volatiles were then removed in a vacuum. The brown residue was extracted with hexane (5 × 20 mL). The combined solutions were filtered, concentrated to 50 mL, and then carbonylated (20 °C, 15 min). The resulting orange solution was concentrated to 10 mL and stored at −30 °C for 16 h to complete the crystallization. The crystals were collected, washed with hexane (2 × 1 mL), and dried in a vacuum to give **3b** (510 mg, 69%) as orange needles: mp 93 °C dec; in solution somewhat sensitive, very soluble in CH_2Cl_2 and toluene, moderately soluble in ether and hexane. Anal. Calcd for $C_{10}H_{14}B_2IRh$: C, 31.14; H, 3.66. Found: C, 30.84; H, 3.69. SIMS (NBA): positive ions, *m*/*z* (I_{rel}) 440 (28, $[Rh_2(C_4H_4BMe)_3]^+$), 386 (100, $[RhI(C_4H_4BMe)_2]^+$), 259 (100, $[Rh(C_4H_4BMe)_2]^+$).

3b: ^{1}H NMR (500 MHz, CD_2Cl_2) δ 5.87 (br, 3-/4-H), 4.13 (m, 2-/5-H), 1.05 (s, Me), and borole signals at 80 MHz 5.86 (m, N = 7.3 Hz, 3-/4-H), 4.14 (m, N = 6.7 Hz, 2-/5-H); $^{13}C\{^1H\}$ NMR (126 MHz, CD_2Cl_2) δ 101.17 (C-3,4), 83.04 (br, C-2,5), 2.74 (br, Me); $^{11}B\{^1H\}$ NMR (CD_2Cl_2) δ 33.

VT-NMR Spectra of 3b: ^{1}H NMR (500 MHz, CD_2Cl_2, −90 °C) C_s isomer (70%) δ 6.03 (m, 3-/4-H) and 4.34 (m, 2-/5-H) for first borole, 5.69 (m, 3-/4-H) and 3.89 (m, 2-/5-H) for second borole, 1.17 (s, Me), 0.61 (s, Me); C_{2v} isomer (30%) δ 5.83 (m, 3-/4-H), 3.93 (m, 2-/5-H), 1.17 (s, 2 Me); $^{13}C\{^1H\}$ NMR (126 MHz, $CDCl_3$, −90 °C) C_s isomer (70%) δ 106.43 [d, ^1J(Rh−C) = 6.0 Hz, C-3,4] and 88.06 (C-2,5) for first borole, 99.25 [d, ^1J(Rh−C) = 6.0 Hz, C-3,4] and 77.17 (C-2,5) for second borole, 4.40 and −1.38 (2 Me); C_s isomer (10%) δ 94.81 [d, ^1J(Rh−C) = 6.1 Hz, C-3,4], 79.53 (C-2,5), 4.67 (Me). Simulation of line shapes: temperature range 193−223 K; signals of all carbons used, ^1J(Rh−C) couplings taken into account, quadrupole broadening of C-2,5 and *B*-Me neglected. $^{11}B\{^1H\}$ NMR (CD_2Cl_2, −90 °C): δ 37 (higher intensity) and 28.

Crystal Structure Determination of 2a, 2b, and 3b. Crystals of **2a** can be obtained from hot toluene solutions. Crystals of better quality were obtained incidentally when a solution of **2a** and **2b** (1/1) in (*E*)-1,2-dichloroethene was cooled to −30 °C. Crystals of **2b** were obtained when a saturated solution in CH_2Cl_2 was cooled from 20 °C to −30 °C. In the case of **3b** the compound was dissolved in the minimum amount of hexane at 20 °C; the solution was kept at −30 °C to give crystals suitable for the structure determination.

The data collection was performed on ENRAF-Nonius CAD4 diffractometers equipped with a graphite monochromator. Crystal data, data collection parameters, and convergence results are given in Table 6.

The major source of systematic error in all three structure determinations stems from absorption: The numerical method by Gaussian integration[27] was used for the crystals of **2a** and **3b** which could readily be face-indexed whereas an empirical absorption correction[28] was applied in the case of **2b**. The structures were solved by direct methods[29] and refined on *F* with the local version of the SDP system.[30] In the final least squares refinements non-hydrogen atoms were assigned anisotropic displacement parameters; in the case of **3b** hydrogen atoms were refined isotropically, whereas the hydrogen atoms were included in riding geometry with fixed displacement parameters (C−H = 98 pm, U_{iso}(H) = 1.3U_{iso}(C)) in the refinement of the structural model for the other compounds.

Acknowledgment. This work was generously supported by Fonds der Chemischen Industrie.

Supporting Information Available: Tables of fractional coordinates of all atoms, anisotropic displacement parameters, and bond distances and angles for **2a**, **2b**, and **3b** (14 pages). Ordering information is given on any current masthead page.[31]

OM970422Q

(27) Coppens, P.; Leiserowitz, L.; Rabinovich, D. *Acta Crystallogr.* **1965**, *18*, 1035.
(28) North, A. C. T.; Phillips, D. C.; Mathews, F. S. *Acta Crystallogr.* **1968**, *A24*, 351.
(29) Sheldrick, G. M. *SHELXS-86, Program for Crystal Structure Solution*; University of Göttingen: Göttingen, Germany, 1986.
(30) Frenz, B. A. ENRAF-Nonius SDP Version 5.0, Delft, The Netherlands, 1989, and local programs.
(31) Further details of the crystal structure analyses are available on request from the Fachinformationszentrum Karlsruhe, Gesellschaft für wissenschaftlich-technische Information mbH, D-76344 Eggenstein-Leopoldshafen, Germany, on quoting the depository numbers CSD-470290 for **2a**, CSD-470291 for **2b**, and CSD-470292 for **3b**, the names of the authors, and this journal citation.